Turkish Journal of Electrical Engineering and Computer Sciences

Volume 18 | Number 3 Article 7

1-1-2010

Nonlinear scattering at HF: Prospects for exploitation in OTH radar systems

STUART ANDERSON

Turk J Elec Eng & Comp Sci, Vol.18, No.3, 2010, © TÜBİTAK
doi:10.3906/elk-1001-396

Nonlinear scattering at HF: Prospects for exploitation in OTH radar systems

Stuart J. ANDERSON
Defence Science and Technology Organisation
PO Box 1500 Edinburgh SA 5111, AUSTRALIA
e-mail: stuart.anderson@dsto.defence.gov.au

Abstract

HF skywave 'over-the-horizon' radars experience exceptionally high levels of clutter from the earth's surface as a consequence of their 'look-down' propagation geometry. While Doppler processing is effective in separating aircraft echoes from the clutter, thereby enabling detection, the same does not always hold for slow moving targets. In particular, ship echoes occupy the same region of Doppler space as the sea clutter, so the likelihood of target echo obscuration is high. By exploiting the known dependence of the characteristic spectral form of the clutter Doppler spectrum on radar frequency and other parameters, HF radars can maximise the prospects for detectability against particular ranges of target parameters. Nevertheless, even assuming that a radar makes use of all available a priori knowledge to optimise its parameters, small ships and boats often escape detection because their echoes are still masked by clutter in the same Doppler subspace. This is particularly likely to occur if the vessels concerned wish to remain undetected, and hence use the properties of sea clutter to their advantage. In this paper we examine the feasibility of a novel approach to the problem of detection against sea clutter – detection via nonlinear scattering mechanisms. The nonlinear scatterers of concern here include electronic systems as well as metal-oxide-metal junctions formed by corrosion in the marine environment. This so-called 'rusty bolt' effect has previously been considered in the context of electromagnetic compatibility of communication systems. Here we explore the possibility of exploiting it to achieve a form of 'clutter-free' radar.

Key Words: *Nonlinear scattering, nonlinear transfer function, Volterra expansion, rusty bolt, HF radar, OTH radar, HFSWR.*

1. Introduction

A defining characteristic of HF skywave 'over-the-horizon' radar is the presence of exceptionally strong clutter from the earth's surface arising from the look-down geometry imposed by reflection from the ionosphere. The presence of this clutter imposes significant demands on the linearity and dynamic range of the radar, In order to detect targets against this clutter background, radars must be able to accommodate signals over a wide

dynamic range without significant distortion, and have the flexibility to operate with parameters which result in a signal-to-clutter ratio high enough to meet detection threshold criteria. The scale of the problem can be illustrated by examining the limits on the key radar parameters:

- The long wavelengths at HF make it exceptionally difficult, if not nigh-impossible, to achieve antenna beamwidths less than 0.1° at feasible cost and with realistic siting constraints. The largest OTH radar systems presently in operation have receive arrays approaching 3 km in length, corresponding to beamwidths in the range 0.2° (at 30 MHz) to 1° (at 6 MHz). At a range of 2000 km, the corresponding cross-range dimension of a resolution cell lies in the range 7–35 km.

- The maximum effective radar waveform bandwidth is limited by a number of considerations, including frequency dispersion, differential polarisation transformation (eg. Faraday rotation), the availability of 'clear' channels in which to operate, apodisation for range sidelobe control, target radar signature characteristics and the frequency dependence of the antenna gain and phase patterns. Typical values for OTH radar bandwidths are 8 – 15 kHz when attempting to detect aircraft and 20 – 50 kHz when searching for ships. The corresponding along-range dimensions of a resolution cell are 10 – 20 km (aircraft mode) and 3 – 8 km (ship mode).

- Combining these numbers, the area of a resolution cell may range from a minimum of 2×10^7 m^2 (73 dBsm) to 7×10^8 m^2 (88 dBsm). The scattering coefficient of the sea surface at HF depends on sea conditions but a representative value for our purposes here is -23 dB [1]. Thus the effective RCS of the clutter contribution from a single resolution cell may lie in the range 50 – 65 dBsm. By comparison, the HF RCS of a fighter aircraft, or a small vessel several tens of metres in length, say, is typically of the order of 20 - 25 dBsm. The corresponding signal-to-clutter power ratio can then be seen to lie in the range -25 to -40 db.

In order to detect targets immersed in such strong clutter, HF radars rely on Doppler processing. For fast targets such as aircraft, the target and clutter subspaces are almost orthogonal, so good separation can be achieved and detection is relatively straightforward. In the case of slow targets, though, the subspaces are not orthogonal: ship echoes are coincident with clutter energy and, depending on target characteristics, sea conditions and the illumination geometry, detectability will be degraded, not infrequently to the point where detection is impossible. Despite this, modern HF radars often perform moderately well against ships, especially large ones. The reason for this success is that the Doppler spectrum of HF radar signals scattered from the sea surface is far from being spectrally white. Most energy is concentrated in discrete peaks, with the residual energy forming a continuum extending to Doppler shifts beyond those associated with typical ship speeds. Figure 1 illustrates the consequences for detection by superimposing representative ship RCS values on a measured clutter spectrum and delineating the resultant 'blind speed' bands.

By exploiting the known dependence of the characteristic spectral form of the clutter Doppler spectrum on radar frequency and other parameters, HF radars can maximise the prospects for detectability against particular ranges of target parameters. Nevertheless, even assuming that a radar makes use of all available *a priori* knowledge to optimise its parameters, small ships and boats often escape detection because their echoes are masked by clutter in the same Doppler subspace. This is particularly likely to occur if the vessels concerned wish to remain undetected, and hence exploit the properties of sea clutter to their advantage. The question arises, is there an alternative domain in which one might separate clutter from target echoes?

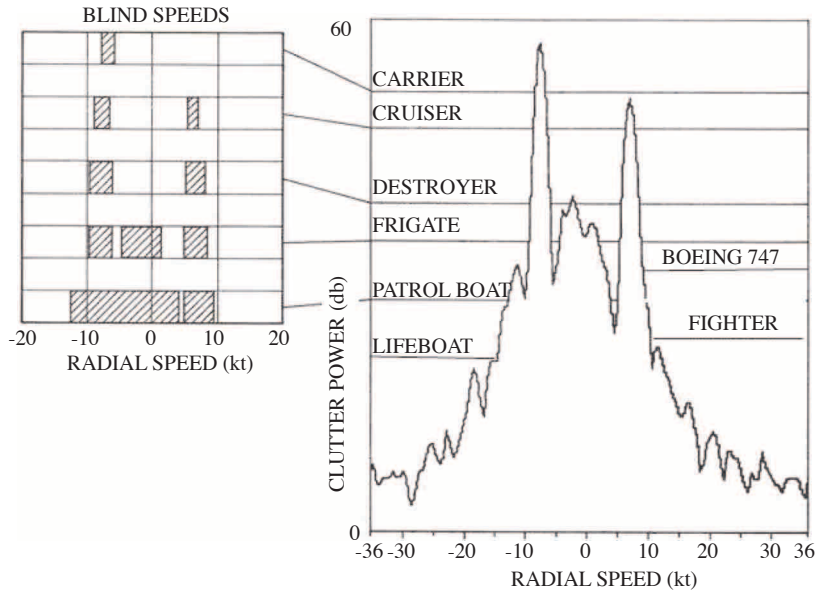

Figure 1. Schematic showing the obscuration of target echoes by low-Doppler clutter under favourable conditions. Target RCS is frequency-dependent, so the levels shown are only indicative.

A hint to a possible approach is the observation that, almost without exception, radar scattering from ships (and aircraft) has been modelled using the approximation of perfectly electrically conducting (PEC) targets. This approximation greatly facilitates the reduction of the radiation integrals to forms which are amenable to solution by the method of moments, and forms the basis of the most widely used HF scattering codes. The most obvious consequence of adopting the PEC assumption is that the predicted RCS will differ from that which would result from an imperfect conductor model for the target constitutive properties. Extensive measurements have shown that the difference is small in most cases, and thus would have little relevance to the problem at hand. A second, more subtle consequence of the PEC assumption is that Maxwell's equations are constrained to be strictly linear. In reality, the constitutive relations of any material scatterer will begin to change as the impressed field strength increases, so Maxwell's equations become essentially nonlinear. It follows that the solutions for the scattered field are characterised by spectral content which differs from that of the incident field. It is this phenomenon that we propose to explore as a means for detecting low RCS targets against the strong clutter background experienced by OTH radar.

The following section discusses nonlinear scattering in the OTH radar context, identifying the principal mechanisms involved. It is advantageous to treat linear and nonlinear scattering in a common framework so in section 3 we review the insightful approach of Hong, Powers and co-workers who adopted the formalism of nonlinear time-invariant systems theory to define a hierarchy of nonlinear radar cross sections (NRCS) [2, 3]. The various NRCS are directly proportional to members of a family of Volterra kernels with a simple but elegant physical interpretation [4-8]. Section 4 uses the resulting generalised radar equation to presents numerical estimates of the achievable signal-to-noise ratios based on second-order statistics, as one might try with conventional radar signal processing tools. The results of this assessment are less than encouraging, so in section 5 we examine HF radar techniques and alternative signal processing schemes which might enhance the detectability of nonlinear echoes. The re-assessment in section 6 establishes the gains that might be achievable

using the techniques of section 5. Finally, in section 7, we discuss some practical issues which would impact on the implementation of a nonlinear echo radar.

2. Nonlinear propagation and scattering at HF

2.1. Sources of nonlinearity

Maxwell's equations in a passive medium can be written in the form

$$\begin{aligned}
&\nabla \times \mathbf{E} + \tfrac{\partial \mathbf{B}}{\partial t} = 0 \\
&\nabla \times \mathbf{H} - \tfrac{\partial \mathbf{D}}{\partial t} = \mathbf{J}_{\text{free}} \\
&\nabla \cdot \mathbf{D} = \rho_{\text{free}} \\
&\nabla \cdot \mathbf{B} = 0
\end{aligned}$$

where $\mathbf{D} = \varepsilon_0 \mathbf{E} + \mathbf{P}$ and $\mathbf{H} = \frac{1}{\mu_0}\mathbf{B} - \mathbf{M}$. These equations constitute a strictly linear system provided that the polarisation $\mathbf{P}$ and magnetisation $\mathbf{M}$ are linearly dependent on the respective fields. For metals and most dielectrics, bulk material properties show a nonlinear field-dependence only under extreme field strengths, so the linear Maxwell's equations describe most everyday electromagnetic phenomena to extremely high precision. Yet, there are configurations of matter which manifest nonlinear responses at moderate or even low field strengths, and three of these are encountered routinely by HF radar [9]. They are (i) plasma media, specifically the ionosphere, (ii) electronic systems and devices containing semiconductor components which are coupled to the illuminating field via cables, casings or antennas, and (iii) metal-oxide-metal junctions, as occur on ships and aircraft. Here our principal concern is with (ii) and (iii), which are localised in the targets.

The potential for generation of intermodulation products (IMP) in passive metallic structures arises predominantly from the physico-chemical processes of metal surface treatment during fabrication and oxidation from exposure to the environment, along with the presence of foreign impurities [10]. The consequence of these mechanisms is the formation of an insulating layer on the surface of each metal component. When two metallic bodies are placed in contact, perhaps bonded by rivets, screws, bolts, welding or soldering, the resulting metal-insulator-metal (MIM) interface is characterised by a current-voltage relationship which departs from linear. The approximate symmetry of the layer relative to the substrates means that the coefficients in the I-V relation,

$$i = a_1 V + a_2 V^2 + a_3 V^3$$

satisfy the condition $a_1 >> a_3 > a_2$.

The application of sealants may mitigate or aggravate the problem. Other passive sources of nonlinearity include coaxial cables and connectors, though these tend to be significantly lower than MIM bonding junctions. A number of investigators have attempted to explain the observed behaviour in terms of quantum tunnelling through a barrier, but the difficulty of modelling the dynamic properties of the barrier in the presence of platform vibration and flexing, as well as the inevitable spatial inhomogeneity, have resulted in poor quantitative agreement with measurements. Hence the most reliable estimates of nonlinear transfer functions derive from measurements.

Other mechanisms which may arise in specific instances include micro-discharge in micro-cracks and across voids, the effects of dirt and surface contamination, high current densities at contacts, nonlinear resistivity of

composite materials and hysteresis effects in ferromagnetic materials. One should also note the widespread introduction of low-observable technologies, including radar absorbing materials. These may achieve their linear echo-reduction objectives at the expense of increasing susceptibility to detection by nonlinear scattering.

Specific shipboard sources of nonlinearity include mooring or anchor chains, expansion joints, cables, slap-down plates, pipe and bracket joints, door hinges, life raft hangers, ladders, armoured cables, LSO nets, antenna guying wires, guard rails, booms, gang planks and roller curtain doors [11]. Nor are aircraft immune from serious electrical nonlinearity, especially where metal panels are bolted or riveted [12], although composite materials are observed to show much lower levels of nonlinear behaviour.

In addition to these unplanned sources of nonlinearity, most aircraft and ships are fitted with numerous electronic subsystems based on semiconductor components, including transmitters, receivers, navigation equipment, loudspeakers, and so on. Apart from the inevitable nonlinearity of real pseudo-linear components, deliberately nonlinear elements are routinely used to protect sensitive receivers from lightning, deliberate jamming and EMP (electromagnetic pulse). If incident radio waves are able to couple into these devices, the probability of nonlinear product generation is high, and that of cross-modulation even higher, so re-radiation may lead to exploitable signals. Coupling may occur via antennas, along cables and wires used for normal signal transmission, or via conducting casings and capacitive effects.

While the consequences of nonlinearity for the platform's electronic systems may be important [13-16], our interest lies in the re-radiation of nonlinear products. Here an important issue arises: at the frequencies of the nonlinear products, the radiation pattern of the re-radiating structure may be quite different from that pertaining to the original incident frequency. Moreover, the radiation resistance will also change. For instance, a half-wavelength centre-fed dipole has a native radiation resistance of 73 Ω but at the second harmonic where it is a one-wavelength antenna, the radiation resistance becomes 2000 Ω. Thus when estimating the susceptibility of a platform to detection by re-radiated signals at harmonic or product frequencies, both inbound and outbound insertion losses must be taken into account.

2.2. A phenomenological model of the re-radiated field

Hong and Powers [2] developed a phenomenological model for the re-radiated field based on the earlier Thevenin equivalent circuit defined by Harger [17, 18] and presented in a modified form in Figure 2.

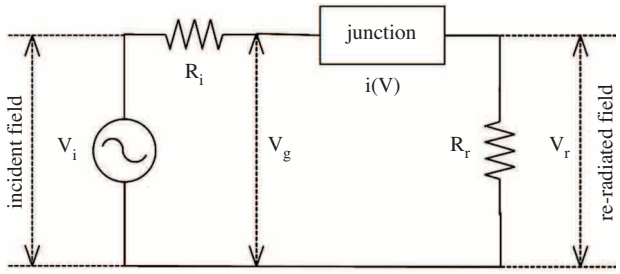

Figure 2. Equivalent circuit for a nonlinear scatterer with current-voltage characteristic I(V).

Following the derivation in [2], but allowing for $a_2 \neq 0$, we have the following relations:

$$I = a_1 (V_g - V_r) + a_2 (V_g - V_r)^2 + a_3 (V_g - V_r)^3$$

$$V_i = IR_i + V_g$$

$$V_r = IR_r,$$

which we solve for the current I to yield an expression for the (memoryless) transfer function which relates the scattered electric field to the incident field. Setting $\mu = R_i + R_r$, the transfer function is given by $V_r = IR_r$ where I satisfies

$$a_3\mu^3 I^3 - \left(a_2\mu^2 + 3a_3\mu^2 V_i\right)\ I^2 + \left(1 + a_1\mu + 2a_2\mu V_i + 3a_3\mu V_i^2\right)\ I - \left(a_1 V_i + a_2 V_i^2 + a_3 V_i^3\right) = 0$$

Knowing the incident power and the nonlinear transfer function enables us to compute the scattered field, as explained in the following section.

3. Systems theoretic representation of nonlinear scattering processes

If a target is illuminated by a radar signal in such a way as to generate a voltage across a component or junction which has a nonlinear voltage-current relation, the resulting currents will re-radiate a scattered field whose spectral content differs from that of the incident field. Although this was recognised in the 1940's and exploited by the 1960's, the adoption of the transfer function formalism from nonlinear systems theory to radar scattering did not occur until 1982 [2]. In this approach, the target can be viewed as an abstract system which acts on an input $x(t)$ to produce an output $y(t)$, and by an obvious extension of the concept of a linear response function, a hierarchy of impulse functions $h_n(t)$ is customarily defined as follows:

$$\begin{aligned} &y(t) = \textstyle\int_{-\infty}^{\infty} h_1(\tau)\, x(t-\tau)\, d\tau \\ &+ \textstyle\int_{-\infty}^{\infty}\int_{-\infty}^{\infty} h_2(\tau_1,\tau_2)\ x(t-\tau_1)\, x(t-\tau_2)\, d\tau_1 d\tau_2 \\ &+ \textstyle\int_{-\infty}^{\infty}\int_{-\infty}^{\infty}\int_{-\infty}^{\infty} h_3(\tau_1,\tau_2,\tau_3)\ x(t-\tau_1)\, x(t-\tau_2)\, x(t-\tau_3)\, d\tau_1 d\tau_2 d\tau_3 + \quad ... \end{aligned}$$

In the OTH radar case, it is more natural to work in the frequency domain; in this case, the nonlinearity is embodied in a hierarchy of nonlinear transfer functions given by the Fourier transforms of the corresponding impulse functions,

$$H_n(f_1, f_2, ...f_n) = \int_{-\infty}^{\infty} ... \int_{-\infty}^{\infty} h_n(\tau_1, \tau_2, ...\tau_n)\ \exp\left[-2\pi i\left(f_1\tau_1 + f_2\tau_2 + ...f_n\tau_n\right)\right] d\tau_1 d\tau_2 ... d\tau_n.$$

The individual contributions to the output signal at n^{th} order of nonlinearity then take the form

$$Y_n(f) = \int_{-\infty}^{\infty} ... \int_{-\infty}^{\infty} H_n(f_1, f_2, ...f_n)\ \delta\left(f - f_1 - f_2 - ... - f_n\right) \prod_{k=1}^{n} X(f_k) df_k.$$

Applying the inverse Fourier transform to each of these yields the corresponding time domain signal component,

$$y_n(t) = \int_{-\infty}^{\infty} ... \int_{-\infty}^{\infty} H_n(f_1, f_2, ...f_n) \prod_{k=1}^{n} X(f_k) \exp\left(2\pi i f_k t\right)\ df_k.$$

The problem with the equation for $y(t)$ in its present form is that it is not a strictly orthogonal representation. This property is inherited by the$Y_n(f)$. In radar practice we are normally concerned with power spectral

density and it is convenient to be able to rely on Parseval's Theorem so, following Hong et al (1980), we modify these equations as follows to enforce orthogonality:

$$\begin{array}{l} y(t) = \int_{-\infty}^{\infty} h_1(\tau)\ (x(t-\tau) - \langle x(t-\tau)\rangle)\, d\tau \\ + \int_{-\infty}^{\infty}\int_{-\infty}^{\infty} h_2(\tau_1,\tau_2)\ (x(t-\tau_1)\,x(t-\tau_2) - \langle x(t-\tau_1)\,x(t-\tau_2)\rangle) d\tau_1 d\tau_2 \\ + \int_{-\infty}^{\infty} h_3(\tau_1,\tau_2,\tau_3)\times \\ \left(x(t-\tau_1)\,x(t-\tau_2)\,x(t-\tau_3) - \sum_{j=1}^{3} x(t-\tau_j)\ \prod_{k=1,k\neq j}^{3} x(t-\tau_k)\right) d\tau_1 d\tau_2 d\tau_3 + \quad ... \end{array}$$

and

$$\begin{array}{l} Y_n(f) = \int_{-\infty}^{\infty} ... \int_{-\infty}^{\infty} H_n(f_1, f_2, ...f_n)\ \delta(f - f_1 - f_2 - ... - f_n)\times \\ \left(\prod_{k=1}^{n} X(f_k) - \sum_{j=1}^{n} X(f_j)\left\langle \prod_{r=1,r\neq j}^{n} X(f_r)\right\rangle\right) \prod_{s=1}^{n} df_s \end{array} .$$

With this formulation, the output power can be written

$$P_y = \langle y^*(t)\ \ y(t)\rangle = \lim_{n\to\infty} \sum\nolimits_{k=1}^{n} Y_k^*(f)\, Y_k(f)\, df,$$

where the termination of the expansion at any order is optimum in the least-squares sense. The incident and scattered power spectral densities of the individual terms at the scatterer are then related by

$$\begin{array}{l} P_y(f) = Y^*(f)\, Y(f) = \int_{-\infty}^{\infty} |H_1(f_1)|^2 P_x(f_1)\ \delta(f - f_1)\, df_1 + \\ \int_{-\infty}^{\infty}\int_{-\infty}^{\infty} |H_2(f_1,f_2)|^2 P_x(f_1) P_x(f_2)\ \delta(f - f_1 - f_2)\, df_1 df_2 + \\ \int_{-\infty}^{\infty}\int_{-\infty}^{\infty}\int_{-\infty}^{\infty} |H_3(f_1,f_2,f_3)|^2 P_x(f_1) P_x(f_2) P_x(f_3)\times \\ \delta(f - f_1 - f_2 - f_3)\, df_1 df_2 df_3 \ + \ \ldots \end{array}$$

since, for a stationary process, $\langle X(f_1)\, X(f_2)\rangle = P_x(f_1)\,\delta(f_1 + f_2)$. The first term on the right hand side of this equation expresses the linearly scattered (output) power at the target as proportional to the incident (input) power with a functional constant of proportionality equal to the squared magnitude of the system transfer function,

$$P_y(f) = |H_1(f)|^2 P_x(f).$$

Assuming an isotropic radiation pattern, if one were to sample this scattered power at a range R_R in the far field with a receiving antenna of gain G_R, the signal power would be given by

$$P_R = \frac{P_y G_R}{(4\pi R_R^2)} \cdot \frac{\lambda^2}{4\pi} \equiv \frac{|H_1|^2 P_x G_R}{(4\pi R_R^2)} \cdot \frac{\lambda^2}{4\pi},$$

where the frequency argument has been suppressed. Suppose now that the incident field at the target is generated by an antenna of gainG_T at range R_T in the far field radiating a total power P_T . Then

$$P_R = \frac{|H_1|^2 P_T G_T G_R \lambda^2}{(4\pi R_T^2)(4\pi R_R^2) 4\pi}.$$

Now, the conventional radar equation states that

$$P_R = \frac{P_T G_T G_R \lambda^2}{(4\pi R_T^2)(4\pi R_R^2) 4\pi}\sigma,$$

where σ is the radar cross section, so we can immediately identify σ with $|H_1|^2$. Hong and Powers [3] proposed that a similar identification can be made between the higher order terms in (7) and a corresponding hierarchy of nonlinear radar cross sections, and proceeded to construct the nonlinear radar equation,

$$P_R(f) = \frac{P_T(f)G_T(f)G_R(f)\lambda^2}{\left(4\pi R_T^2\right)\left(4\pi R_R^2\right)4\pi}\sigma_1(f) +$$
$$+ \iint \frac{P_{T_1}(f_1)G_{T_1}(f_1)P_{T_2}(f_2)G_{T_2}(f_2)G_R(f)\lambda^2}{\left(4\pi R_{T_1}^2\right)\left(4\pi R_{T_2}^2\right)\left(4\pi R_R^2\right)4\pi}\delta(f - f_1 - f_2)\sigma_2(f_1, f_2)\,df_1 df_2 +$$
$$+ \iiint \frac{P_{T_1}(f_1)G_{T_1}(f_1)P_{T_2}(f_2)G_{T_2}(f_2)P_{T_3}(f_3)G_{T_3}(f_3)G_R(f)\lambda^2}{\left(4\pi R_{T_1}^2\right)\left(4\pi R_{T_2}^2\right)\left(4\pi R_{T_3}^2\right)\left(4\pi R_R^2\right)4\pi}\delta(f - f_1 - f_2 - f_3)\cdot$$
$$\sigma_3(f_1, f_2, f_3)\,df_1 df_2 df_3 \quad + \ ...$$

Note that multiple transmitters T_k are accommodated in this model so as to match the proposed OTH radar configurations. By referring the RCS to the actual measurement at the radar receiver, rather than at the target, this equation provides the model for experimental measurements.

4. Estimating nonlinearly scattered fields at HF

4.1. Lessons from shipboard communications systems

As a guide to what might be possible with HF radar, it is of interest to examine the experience of ship-board HF communications systems. According to numerous studies and reports from naval personnel, the IMD problem on ships is acute: nonlinear products at low order may be comparable in power with weaker primary signals, while higher orders have been observed to be significant up to 21^{st} order and detectable to more than the 50^{th} order. They can have significant operational implications on system availability. Further, the number of IMD frequencies generated increases dramatically with the number of emitters, so the resultant background IMD level on board a ship with several co-active transmitters is typically 30–60 dB above the quasi-minimum noise floor, as illustrated in Figure 3. So serious is the problem that US Navy ships are said to be 'clean' if the 19^{th} order nonlinear interference products are not detectable above the noise floor.

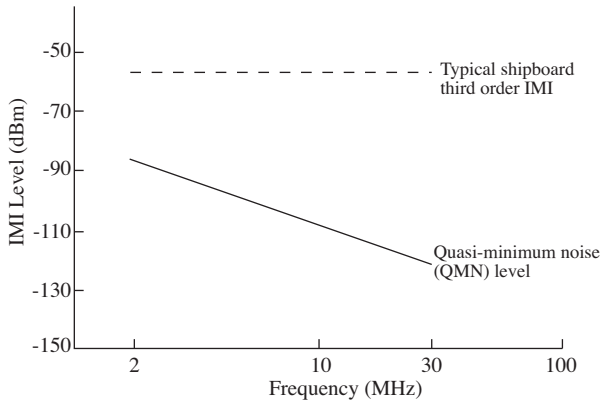

Figure 3. Typical shipboard intermodulation interference (IMI) levels compared with quasi-minimum noise [19].

We can estimate an effective nonlinear intercept for use in NRCS calculations by taking the power levels reported by Cooper et al [11], who assumed a transmit power of 1 kW, a 5 dB mismatch loss and a 30 dB

propagation loss to a single 'rusty bolt' representative of those identified during a ship survey at 100 MHz, yielding a power flux density of +25 dBm. In their example the conversion to inter-modulation products incurred a 36 dB loss, and as the metal-oxide-metal junction is approximately symmetric, we can infer that the IMD was dominated by third order terms. Accordingly, the third order intercept for the single 'rusty bolt' was $\sim$ +37 dBm. This needs to be scaled by the effective number of such nonlinearities, which, based on nonlinear product levels, might lie in the range 10^2 –10^3.

4.2. Order of magnitude estimates of nonlinearly scattered fields

4.2.1. HF skywave radar

First, an important point: it is often the case that the prevailing propagation modes do not support both second- and third-order product frequencies. In Figure 4, both are received as there is a sporadic-E layer which supports the sum frequency to the same group delay. This contrasts with Figure 5, where only the F-layer is present; here the sum frequency does not propagate from the target back to the radar receiver, assumed to lie at the same range as the transmitters, about1100 km. On the other hand, third-order products can be controlled to lie arbitrarily close to the propagating frequencies, so this product is in principal always available.

Using representative values for a typical large skywave radar, illuminating a destroyer-sized ship and assuming a radio-quiet location with the background noise floor at 15 dB above thermal noise, we obtain the *linear*, *quadratic* and *cubic* echo signal-to-noise ratios plotted in Figure 6. Clearly there is little prospect for successful detection via the nonlinear returns.

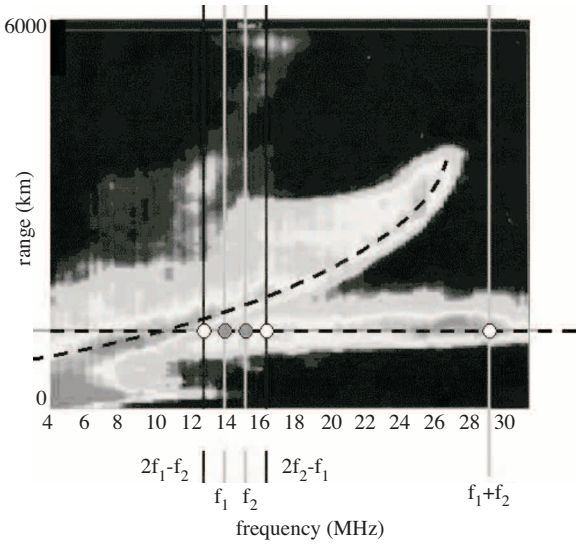

Figure 4. Primary frequencies and their low-order nonlinear products superimposed on a backscatter ionogram when sporadic-E is present.

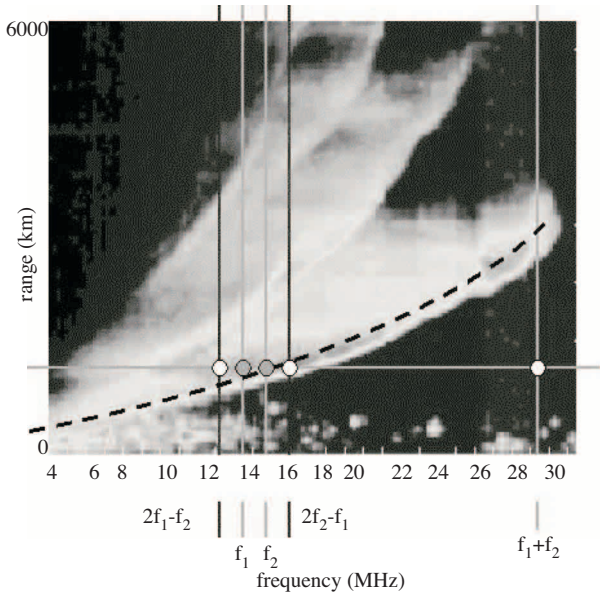

Figure 5. Primary frequencies and their low-order nonlinear products superimposed on a backscatter ionogram when only F-layer propagation is present.

4.2.2. HF surface wave radar

Now consider a military HFSWR comparable to the Australian SECAR radar [1], with a power of 5 kW, operating against a destroyer-sized target at a range of 100 km. The radar frequency is chosen to be 5 MHz, sweeping across a 20 kHz bandwidth. This yields a field strength in excess of 3 mV/m at the target. Substituting in the nonlinear radar equation, with conventional processing based on second-order statistics, we obtain the SNR predictions shown in Figure 7.

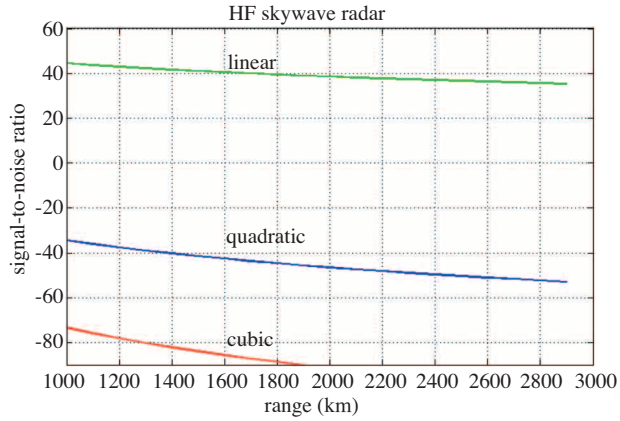

Figure 6. Signal-to-noise ratio versus range for a skywave radar illuminating a destroyer. Linear, quadratic and cubic nonlinear echoes are shown.

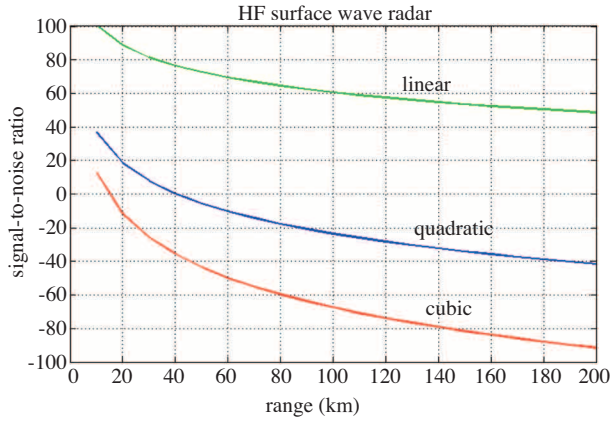

Figure 7. Signal-to-noise ratio versus range for an HFSWR illuminating a destroyer. Linear, quadratic and cubic nonlinear echoes are shown.

These results indicate that conventional HFSWR processing will not yield a useful nonlinear echo detection capability, though such echoes may be observed at short ranges.

5. Techniques for enhancing nonlinear echoes

5.1. Choice of waveforms: carrier frequency

Just as the linear HF RCS of any target shows a frequency dependence, so will the NRCS terms. In principle one might take advantage of this to enhance detectability via the NRCS, but given the constraints on choice of carrier frequency imposed by propagation considerations, this avenue may be difficult to exploit in practice. Still, it is certainly worth detailed investigation. One might seek in particular to maximise the driven currents associated with target resonances.

It would also seem important to choose the carrier frequency so that the frequency of the nonlinearly scattered field to be used for detection lies in a region of the HF spectrum where the background power spectral density is low. This consideration must be qualified by the fact that the background noise, or at least, the Gaussian part thereof, can be reduced by the higher-order spectrum analysis techniques described below.

5.2. Choice of waveforms: modulation

The use of a continuous waveform such as linear FMCW has the advantage of avoiding any need for pulse chasing. As mentioned earlier, the need to separate the collaborating transmitters means that synchronisation

is a critical issue, being range- and direction-dependent. On the other hand, use of pulse waveform with a fractional duty cycle γ but the same average power results in a nonlinear scattered field gain of $\gamma^{-n/2}$ for the NRCS of order n. Thus for the cubic NRCS and a 25% duty cycle, the gain is a factor of 8 or 9 dB.

Assuming for the moment that the waveform architecture is decided, we mention that the optimum choice of illumination frequencies is not arbitrary but has a well-defined structure [20].

5.3. Ionospheric focussing

HF propagation occurs within the curved earth-ionosphere waveguide so, as with optical reflection from a curved mirror, the electromagnetic field experiences focussing and defocusing, as well as the formation of caustics. There are three main types of focussing: antipodal focussing, horizon focussing and layer focussing [21-23]. The first is of little interest for the present study, as it does not offer the potential for controlled movement and is, in any event, imperfect, and located in the region most distant from the radar. The second tends to achieve its greatest concentration of energy at low grazing angles, and offers limited control, but nonetheless may have limited applications. Of greatest potential is layer focussing, where knowledge of the specific vertical profile of the refractive index can be exploited to achieve substantial focussing by adjusting the radar beam pattern, waveform and carrier frequency. A suboptimum form of this focussing is ubiquitous in backscatter ionograms, at the skip distance.

The importance of focussing here is the prospect of increasing the field strength at the target, thereby magnifying the nonlinear effects. Simple models of layer focussing have been derived for canonical electron density profiles over a flat earth, but these often lead to predicted singularities in the field. Here we have derived an expression for the focussing gain using a much more realistic model: a spheroidal earth and a quasi-parabolic layer profile, as widely used in coordinate registration schemes for OTH radar. The power flux is given by the Poynting vector,

$$\mathbf{S} = \mathbf{E} \times \mathbf{H},$$

so, near the earth's surface, we can express the magnitude of the Poynting vector by

$$S = \frac{kE^2}{\omega\mu_0} = \sqrt{\frac{\varepsilon_0}{\mu_0}}E^2 = \frac{E^2}{Z_0},$$

where $Z_0 \approx 377\Omega$ is the characteristic impedance of free space. Assuming an antenna radiating 1 kW isotropically into a half-space, the electric field strength just above the surface for one-hop illumination at take-off elevation angle α is

$$|E| \approx 2.5 \times 10^5 \tan\alpha \cdot \left[R_g \cdot \left|\frac{\partial R_g}{\partial \alpha}\right|\right]^{\frac{1}{2}} mV/m$$

where R_g is the ground range. Figure 8 illustrates the bunching of rays near the skip distance.

Measurements have found that both horizon focussing and layer focussing are capable of delivering power density gains of the order of 10 dB, limited ultimately by small-scale ionospheric structure. The HF broadcast community does not exploit these peak gains as they apply to only a localised region near the skip distance; broadcasting seeks to maintain stable, wide area illumination at a fixed frequency. In our application, achieving the maximum focussing gain is the goal.

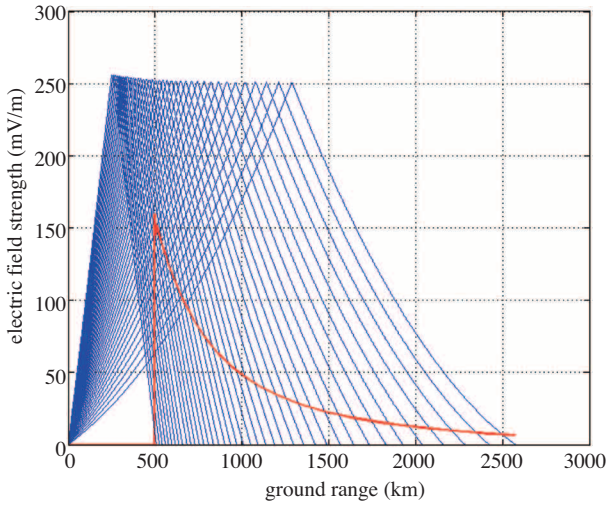

Figure 8. A typical HF ray fan with the electric field strength profile overlaid to show skip focussing.

5.4. Signal processing using higher-order spectrum analysis

From the preceding examples, it is evident that detection based on second order statistics, that is, power spectra and cross spectra, may be marginally viable for HFSWR but falls far short of viability for HF skywave radar. This conclusion is valid as stated, but it overlooks the intriguing idea of using nonlinear signal processing when seeking nonlinear signals. Specifically, the power spectrum ratios customarily used for detection in conventional radar signal processing can be abandoned in favour of detectors based on higher order statistics in the bispectrum or trispectrum domains. This idea was pioneered by Hong and Powers [3] who showed that for weakly nonlinear metallic targets, gains in detectability of tens of dB could be achieved. The key idea is that the phases of the nonlinear products are coherent with those of the primary incident fields, so by performing the corresponding orders of cross-spectrum analysis, the weak nonlinear echoes can be integrated coherently, with associated processing gain relative to the (uncorrelated) noise. In particular, the higher-order spectra of Gaussian noise tends to zero, which is a property worth keeping in mind when choosing radar frequencies. Estimation of cross spectra can conveniently be implemented in the signal processing at the receiver in terms of products of the DFTs of the transmitted and received signals [9]. Thus, for instance, computation of the cross trispectrum in the non-degenerate case yields the third-order cross section

$$\sigma_3(f_1,f_2,f_3)=\left|\frac{1}{3!}\frac{\langle Y(f_1+f_2+f_3)\,X^*(f_1)\,X^*(f_2)\,X^*(f_3)\rangle}{\left\langle |X(f_1)|^2\,|X(f_2)|^2\,|X(f_3)|^2\right\rangle}\right|^2,$$

and this same statistic can be used for target detection. For narrow band radar signal spectral support, as is generally the case with OTH radar, the nonlinear radar cross section may be assumed independent of frequency and thus averaging can take place over the Fourier transform index.

6. Revised estimates of NRCS detectabilty

In view of the prospect of exploiting ionospheric focussing to advantage and the much increased processing gain achievable through the use of higher-order cross spectral density estimation, it is worth revisiting the estimates of Section 4. Suppose that a focussing gain of 10 dB is possible on each illumination path but to be conservative ignore the possibility of focussing gain on the receive path. Further, assume that joint path coherence can be maintained over a period of 100 seconds, as has been demonstrated during observations of targets and sea clutter with the Jindalee OTH radar, with slow time samples at 5 Hz. Following Hong and Powers [3], we assume a additional processing gain of 20 dB by analysing the signal in the cross-trispectrum domain. This processing gain is assumed for both skywave OTH radar and HFSWR. With these assumptions, we re-compute the SNR curves plotted in Figures 6 and 7, obtaining the revised curves plotted in Figures 9 and 10.

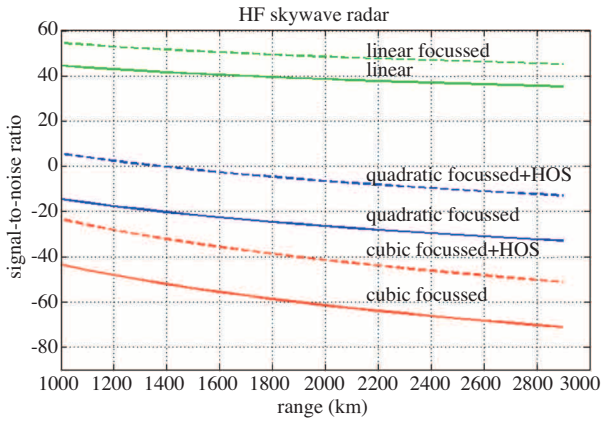

Figure 9. Signal-to-noise ratio versus range for a skywave radar illuminating a destroyer. Linear, quadratic and cubic nonlinear cases are shown for two cases: (i) skip-focussed, and (ii) skip-focussed together with HOS processing.

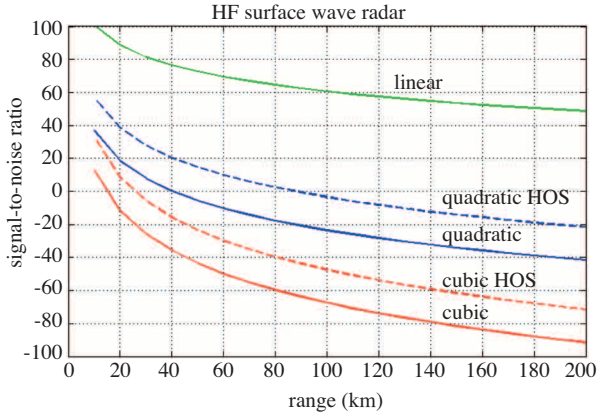

Figure 10. Signal-to-noise ratio versus range for an HFSWR illuminating a destroyer. Linear, quadratic and cubic nonlinear cases are shown for both standard processing and HOS processing.

Clearly there is now some scope for optimism, though we stress that these curves are based on the assumption of a nonlinear junction characteristics with quadratic nonlinearity coefficient of 10^{-3} times the linear coefficient and cubic nonlinearity coefficient of 10^{-2} times the linear coefficient. One needs to conduct measurements of ships to make a reliable assessment of cumulative nonlinearity, but the chosen values do not seem ridiculously high.

7. Other factors influencing viability of NRCS detection

7.1. Internal radar system nonlinearity

Modern direct synthesis digital waveform generators achieve their outstanding flexibility without incurring a significant penalty in terms of phase noise, but they can suffer from low levels of harmonic distortion. The same problem arises with the power amplifiers, but as the power gain here is typically in the range 30 – 50 dB, the harmonic distortion can be much more serious. Solid-state amplifiers are implemented via a modular structure

to reduce the potential for unwanted distortion, but even so, measurable levels of nonlinear products are often present. Fortunately, such nonlinearity as occurs tends to be memoryless and therefore results predominantly in the generation of harmonics of the instantaneous signal frequency. Thus, while these components theoretically have the potential to mask harmonic scattering originating from nonlinear targets, they do not impact on other, more general scattering scenarios as discussed below. In practice the problem is mitigated by the filtering inherent in skywave propagation where the illumination is optimised for the fundamental carrier frequency. Further rejection arises from the cross-ambiguity function processing at the receiver and, optionally, the insertion of a sub-octave anti-aliasing filter in the receiver front end. Transmitting antennas are potentially a greater source of nonlinearity, especially at high power levels where arcing can occur, but even here the distortion is generally low. Moreover, as it is associated with impulsive noise which is likely to be detected and removed by corrective signal processing, essentially a time domain filter, the transient burst of harmonics should be suppressed along with the noise. It is appropriate to point out that Aeolian vibration of the antenna, whilst capable of introducing an unwanted modulation on the signal, is not a nonlinear mechanism – it is bilinear.

At the receive site, potential intermodulation distortion inside modern digital receivers is kept to acceptable levels by careful hardware design, preferably aided by astute choice of radar operating frequency to avoid cross-modulation products and reciprocal mixing associated with powerful radio broadcast signals in adjacent frequency bands [1].

7.2. Near-field external nonlinearity

There is always some potential for nonlinear scattering in the vicinity of radar transmit sites, including that from buildings, fences, towers, masts, unshielded electronic equipment and road traffic, but again, this is likely to consist primarily of harmonics of the radar signal frequency. In addition, such scattering is most unlikely to be coupled to an effective radiator, directional and aligned with the radar transmit beam, so its consequences may be assumed to be negligible. Some possibility of cross-modulation involving other signals may exist as OTH radar transmit facilities are not always located in such electrically quiet zones as those selected for OTH radar receive sites.

7.3. Propagation through the nonlinear ionospheric plasma medium

It is in the ionospheric plasma that serious levels of nonlinearity occur, as first observed by Tellegen in 1933 [24]. There are many forms of nonlinearity which can occur during ionospheric propagation, and typically these start to become significant at field strengths of the order of 10^{-1} V/m in the F-region, easily achieved with a large OTH radar with perhaps 55 dBW transmit power and more than 25 dB directive gain.

Nonlinearity during skywave propagation is of practical relevance to HF radar in three ways: first as a means of heating the ionosphere to modify its refractive and absorptive properties for subsequent exploitation, second as a means of transferring modulation from one signal to another – the Luxembourg-Gork'ii effect, and third because of the potential for self-focussing and self-modulation. Yet, as ionospheric nonlinearity does impact on the ability of different OTH radar configurations to associate the nonlinear echoes unambiguously with the target, we make the following brief commentary.

The simplest form of nonlinearity arises because the plasma dielectric tensor is field-strength dependent, being a function of the electron-neutral collision frequency, which itself depends on the electron temperature and thus on the action of the electric field of the incident radiowave. Provided that the electromagnetic field

does not approach extreme intensities, it is reasonable to postulate that the field dependence of the constitutive parameters of a medium can be expressed in power series form.

Following Censor [25], we can introduce nonlinear constitutive relations via a hierarchy of terms,

$$\mathbf{D} = \mathbf{D}^{(1)} + \mathbf{D}^{(2)} + ... + \mathbf{D}^{(n)} + ...$$
$$\mathbf{D} = \mathbf{D}^{(1)} + \mathbf{D}^{(2)} + ... + \mathbf{D}^{(n)} + ...$$

where the leading terms represent the linear behaviour.

In order to preserve generality of the response, it is advantageous again to employ the Volterra series expansion:

$$\mathbf{D}_j^{(n)}(\mathbf{X}) = \int d^4\mathbf{X}_1 ... \int d^4\mathbf{X}_n \left[\varepsilon_{ij...m}^{(n)}(\mathbf{X}_1, \mathbf{X}_2, ...\mathbf{X}_n)\, \mathbf{E}_j(\mathbf{X} - \mathbf{X}_1) ... \mathbf{E}_m(\mathbf{X} - \mathbf{X}_n)\right]$$

where $i, ... m = 1,2,3$ denote Cartesian coordinates and $\mathbf{X} \equiv (x_1, x_2, x_3, ict)$. Thus, for $n = 1$,

$$\mathbf{D}_j^{(1)}(\mathbf{X}) = \int d^4X_1\, \varepsilon_{ij}^{(1)}(\mathbf{X}_1)\, \mathbf{E}_j(\mathbf{X} - \mathbf{X}_1)$$

with space-time Fourier transform

$$\mathbf{D}_j^{(1)}(\mathbf{K}) = \varepsilon_{ij}^{(1)}(\mathbf{K})\ \mathbf{E}_j(\mathbf{X} - \mathbf{X}_1)$$

The dependence of ε on $\mathbf{K}$ accounts for dispersion. Specific expressions for $\varepsilon_{ij}^{(1)}(\mathbf{K})$ depend on the plasma model adopted [26].

If we adopt a plane wave ansatz for $\mathbf{E}(\mathbf{X})$, it is clear that the products of fields appearing in the terms where n¿1 will correspond to harmonics of the fundamental wave. Moreover, if several plane waves are taken as the primary field, cross terms at all product frequencies are inherently possible. Thus the nonlinear medium has the effect of 'mixing' the impressed fields and generating a spectrum of nonlinear product waves. This phenomenology is precisely what we are relying on the target to exhibit, so that it can be detected, hence it is evident that the radar observation process must be structured in such a way as to ensure that nonlinear echoes from the target are not contaminated with nonlinear signals from other mechanisms. A suitable configuration is described in section 7.4.

An order of magnitude estimate of the ratio of the second harmonic power to that of the fundamental can be obtained by a one-dimensional numerical integration of Maxwell's equations using a single fluid model of electron density, as carried out by Eliasson and Thide [27] for the case of an amplitude-modulated broadcast signal at vertical incidence. Their computation yielded a value in the vicinity of -12 dB, which is certainly significant. Now, the efficient excitation of most important nonlinear processes in the ionosphere is achieved near vertical incidence, so this result is not directly applicable to oblique propagation. Still, even allowing for substantially reduced effects in a more realistic skywave radar geometry, it suggests harmonic generation at a level much higher than that likely to be produced by a typical nonlinear target in the OTH radar footprint.

7.4. Implications for detection of nonlinear target echoes

From the preceding discussion it is fairly evident that the detection of nonlinear target echoes requires a measurement configuration which avoids or at least minimises the generation of nonlinear products by mechanisms

other than scattering from the target itself. We can summarise the implied constraints on the design of an HF radar system attempting to detect nonlinear echoes as follows:

1. harmonics arise in many ways so they may not be the best class of nonlinear echoes to exploit; and
2. the ionosphere is pervaded by HF signals and any two which traverse the same volume of space will generate nonlinear products.

It takes no great insight to see that these constraints are compatible with a radar configuration consisting of two widely separated transmitters and a single receiver which, preferably, is distant from both transmitters. In the simplest implementation, the transmitters would operate on separate carrier frequencies, f_1 and f_2, say, and the receiver would be tuned to either of the third-order products, $2f_1 - f_2$ and $2f_2$ - f_1. By judicious choice of the separation $|f_1 - f_2|$, one of the third order products could be tuned to optimise skywave propagation conditions from the target to the receiver. Harmonics of the two carrier frequencies are trivially avoided and the two distinct skywave paths from the transmitters to the target would not intersect in the ionosphere where mixing would otherwise occur.

While this solution is fine in principle, the issue of joint availability of suitable frequencies for transmission and reception should not lightly be dismissed. For a start, the illuminating frequencies need to be close to the maximum operating frequencies for their respective paths, so as to achieve peak power density at the target. The product frequencies need to be similarly matched to the path from target to receiver. Based on observations of the diurnal variability of skywave propagation and, in particular, the statistics for instantaneous range depth [7] and for joint frequency availability [5], it seems clear that meeting these conditions would not always be possible. The detection of second-order nonlinear echoes required a relatively non-dispersive propagation path, which is often present in the form of a sporadic-E layer, so this is an avenue worth experimental investigation, though such layers usually allow significant transmission. For third order NRCS, the higher reflectivity of the F2 layer is to be preferred. In this case, a second, more subtle consideration is the spectral broadening of the nonlinear products which arises from the intervention of various plasma wave species in the wave–plasma interaction. Typically these modulate the harmonics by 40 – 60 kHz. This sets a limit on the closeness of the carrier frequencies of the radar signals being used to generate the nonlinear product terms at the scatterer.

8. Conclusions

The 'back-of-the-envelope' calculations in this paper suggest that the goal of detecting nonlinear echoes from ships, at least, may not lie beyond the capabilities of HF skywave radar, and almost certainly is possible with HFSWR at useful ranges. There is also the prospect of a contribution to target classification at HF [28].

While the achievable SNR may be modest, the gains to detectability of slow targets by eliminating sea clutter are so large that the feasibility of nonlinear HF radar seems worthy of closer examination.

References

[1] Headrick, J.M., and Anderson, S.J., 'HF Over-the-Horizon Radar', Chapter 20, *Radar Handbook*, Merrill Skolnik, (Ed.), 3^{rd} edition, February 2008.

[2] Hong, J.Y.; Powers, E.J., 'Digital signal processing of scattering data from nonlinear targets', in Proceedings of the IEE International Conference, Radar '82, London, October 18-20, pp.266-270,1982.

[3] Hong, J.Y.; Powers, E.J., 'Detection of weak third harmonic backscatter from nonlinear metal targets', in Proceedings of the Sixteenth Annual Electronics and Aerospace Conference and Exposition, EASCON '83, Washington, DC, September 19-21, pp.169-175, 1983.

[4] Powers, E.J.; Ritz, C.P.; An, C.K.; Kim, S.B.; Miksad, R.W.; Nam, S.W., 'Applications Of Digital Polyspectral Analysis To Nonlinear Systems Modeling and Nonlinear Wave Phenomena', Workshop on Higher-Order Spectral Analysis,
28-30 June, pp.73 – 77, 1989.

[5] Nam, S.W., Kim, S.B., and Powers, E.J., 'Utilization of digital polyspectral analysis to estimate transfer functions of cubically nonlinear systems with nonGaussian inputs', IEEE International Conference on Acoustics, Speech, and Signal Processing, ICASSP-89, Glasgow, Vol.4, pp. 2306-2309, 1989.

[6] Im, S., Kim, S.B., and Powers, E.J., 'Orthogonal development of a discrete frequency-domain third-order Volterra model', Proceedings of the IEEE International Conference on Acoustics, Speech, and Signal Processing, ICASSP-93, Minneapolis, Vol. 4, pp. 484-487, 1993.

[7] Im, S., Kim, S.B., and Powers, E.J., 'Utilization of orthogonal higher-order coherence functions for cubic Volterra model identification', Workshop on Higher-Order Statistics, pp.116 – 120, 1993.

[8] Powers, E.J., and Im, S., 'The utilization of higher-order spectra to determine nonlinear radar cross sections', Proceedings of the IEEE International Conference on Acoustics, Speech, and Signal Processing, ICASSP-94, Adelaide, Vol. 4, pp. 437-440, 1994.

[9] Anderson, S.J., Mahoney, A.R., and Zollo, A.O., 'Applications of Higher-Order Statistical Signal Processing to Radar', pp.405 – 446 (Chapter 13) in '*Higher-Order Statistical Signal Processing'*, B. Boashash, E.J.Powers and A.M.Zoubir, (Ed.), Longman Australia and Halstead Press, 1995.

[10] Shands, T.G., and Woody, J.A., 'Metal-insulator-metal junctions as surface sources of intermodulation', RADC Technical Report RADC-TR-83-31, February 1983.

[11] Cooper, J.C., and Panayappan, R.,'Chemically Suppressing Rusty-Bolt Intermodulation Interference', Proc. IEEE National Symposium on EMC, April, 1984, pp. 233-240.

[12] Watson, A.W.D., 'The measurement, detection, location and suppression of external non-linearities which affect radio systems', in Proceedings of the Conference on Electromagnetic Compatibility, Southampton, England, September 1980, pp. 1-10, 1980.

[13] Nosek, L.T., 'Hull-generated intermodulation interference: an insidious electromagnetic compatibility foe', Naval Engineers Journal, Vol.109, No.3, pp. 331-338, May 1997

[14] Betts, J.A., and Ebenezer, D.R., 'Intermodulation interference in mobile multiple-transmission communication systems operating at high frequencies (3 – 30 MHz)', Proceedings of the IEE, Vol.120, No. 11, pp.1337 – 1344, November 1973.

[15] Mieth, W.B., 'A cost-effective solution to measurement of hull-generated intermodulation interference on U.S. Navy ships', National Symposium on Electromagnetic Compatibility, USA, May 1989, pp.186-189, 1989.

[16] Elsner, R.F., Frazier, M.J., Smulhstys, L.S., and Wilson, E., 'Environmental interference study aboard a naval vessel', Proceedings of the IEEE Electromagnetic Compatibility Symposium., pp. 330-338, 1968.

[17] Harger, R.O., 'Harmonic radar systems for near-ground in-foliage nonlinear scatterers', IEEE Trans, Aerospace and Electronic Systems, Vol.AES-12, No.2, pp. 230-245, March 1976

[18] Harger, R.O., and Lewinski, D.J., 'Nonlinear effects of negative resistance amplifiers on signals', Proc. IEEE, Vol.55, p.1507, August 1967

[19] Hynes, R., Carhart, H.W., and Cooper, J.C., 'Chemical reduction of intermodulation interference caused by metal-oxide-metal junctions aboard ship', NRL Report 9344, July 1991

[20] Victor J.D., and Knight, B.W., 'Nonlinear analysis with an arbitrary stimulus ensemble', Quarterly of Applied Mathematics, Vol. 37, No.2, pp.113-136, July 1979.

[21] Kelso, J.M., 'Radio ray propagation in the ionosphere', McGraw-Hill, 1964, pp. 257-260.

[22] Humphrey, L.C., 'Horizon focusing effects observed on ionospherically reflected radio waves', Radio Science, Vol.3, no. 11, November 1968.

[23] Bradley, P.A., 'Focusing of radio waves reflected from the ionosphere at low angles of elevation', Electronics Letters, Vol.6, No.15, 23 July 1970, pp.457-458

[24] Hill, J.R., 'Exact ray paths in a multisegment quasi-parabolic ionosphere, Radio Science, Vol.14, No.5, pp.855-861, Sept-Oct. 1979.

[25] Tellegen, B.D.H., 'Interaction between radio waves?', Nature, Vol.131, 840,1933.

[26] Censor, D., 'Scattering from weakly nonlinear objects', SIAM Journal of Applied Mathematics, Vol.43, No.6, pp. 1400-1417, December 1983.

[27] Maslin, N.M., 'Estimating ionospheric cross-modulation', Proc. R. Soc. Lond. A 351, 277-293, 1976.

[28] Eliasson, B., and Thidé, B., 'Simulation study of the interaction between large-amplitude HF radio waves and the ionosphere', *Geophys. Res. Lett.*, 34, L06106, 2007.

[29] Anderson, S.J., 'Target classification, recognition and identification with HF radar, Proceedings of the NATO Research and Technology Agency *Sensors and Electronics Technology Panel Symposium SET-080/RSY17/RFT 'TARGET IDENTIFICATION AND RECOGNITION USING RF SYSTEMS'*, Oslo, Norway, October 2004.